EFFECTS OF INSERTION DEVICES ON STORED ELECTRON BEAM OF HIGH ENERGY PHOTON SOURCE*

X.Y. Li [†], D.H. Ji, Y.Jiao, Z. Duan, Y.F. Yang, Key Laboratory of Particle Acceleration Physics and Technology, Institute of High Energy Physics, Beijing 100049, China

Abstract

The High Energy Photon Source (HEPS) is a 4th generation, 6-Gev, ultralow-emittance, photon source project in China. High brightness hard X-ray beams at the energy particularly above 10kev are provided by insertion devices installed in straight sections of the storage ring. Brightness tuning curves of 14 ID beamlines planned in HEPS first stage are obtained after designing their parameters. However the presence of these insertion devices produce several effects on the beam performances including betatron tunes, betatron amplitude functions, closed orbit, emittance and dynamic aperture etc. It is found that the vertical octupole effect due to the fourteen IDs under the present schemes produce the most significant effect on the vertical dynamic aperture reduction. The ID field error effects on close orbit can be completely compensated by two correctors adjacent the ID at the both side. The horizontal emittance reduces to 36pm.rad due to the damping wiggler effect of IDs with field error after the orbit correction is also obtained.

INTRODUCTION

It is plan to build 14 beamlines for SR users in the first-stage of HEPS project. Multiple insertion devices including cryogenic permanent magnetic undulator (CPMU)[1], APPLE-II type of ellipse polarization undulator[2], in air planar undulator(IAU) and wiggler are applied to satisfy different user requirements.

Table.1: Main Parameters of IDs for 14 Beamlines

Name	Energy range	B Min(T)	B Max (T)	λ u (m)	Nu
CPMU13.5	7~10keV/ 17-	0.29	0.90	0.0135	155
CPMU17	18/51-53kev	0.29	1.23	0.0170	123
CPMU18	5~70keV	0.29	1.36	0.0184	228
CPMU15	40~100keV	0.29	1.10	0.0155	271
CPMU18	5~60keV	0.29	1.36	0.0184	228
EPU73	0.05~2keV	0.22	2.0	0.0725	69
IAU32	1.75~8keV	0.22	1.0	0.0328	153
IAU28	4~30keV	0.22	0.85	0.0282	177
IAU28	5~18keV	0.22	0.85	0.0282	177
IAU28	5~50keV	0.22	0.85	0.0282	177
IAU28	6~25keV	0.22	0.85	0.0282	177
IAU28	5~23keV	0.22	0.85	0.0282	177
IAU28	10~50keV	0.22	0.85	0.0282	177
IAU22	8keV	0.22	0.63	0.0227	220
IAU32	2~20keV	0.22	1.0	0.0319	156

For the 6m straight section of HEPS storage ring

scheme at present, the length of in air undulator is 5m and the minimum gap is 9mm while the CPMU is 2.1m long with 5mm minimum gap. We assemble the two CPMU in tandem on one straight section with a phase shifter between them for one beamline. Parameters of IDs are general-purposed and determined after collecting the requirements of all users. Most of in air undulators are standardized on the 28.2mm-period undulator for the requirement of photon energy should continuously tunable. Main parameters of IDs of 14 beamlines are listed in table 1.

BRIGHTNESS OF PHOTON SOURCES

The brilliance $B(\vec{x},\vec{x}',s,w)$ of a SR source is an invariant in any ideal optical photon beam transport system which represents the phase space density of photon flux with the frequency w. It is a fundamental property of SR source so that one can derive any other SR quantity from brilliance. The unit of the brilliance is the number of photons per second, per 0.1% spectral bandwidth, per unit solid angle and per unit source size.
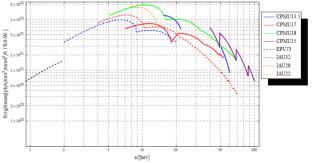
The general definition of the brilliance was first introduced by K.J.Kim from the electric field by means of the Wigner distribution function.[3] With such definition, the brilliance is expressed in terms of the dimensionless vector $\vec{H}$ [4] in the case of far-field approximation.
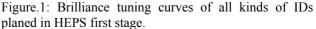
$$B(\vec{x},\vec{x}',s,w) = \frac{\alpha d}{e}\left(\frac{w}{2\pi c}\right)^2 \int\int\int_{-\infty}^{\infty}\left(\vec{H}\left(\vec{x}'+\frac{\vec{\xi}'}{2},w\right)\vec{H}^*\left(\vec{x}'-\frac{\vec{\xi}'}{2},w\right)\right)\exp\left(-i\frac{w}{c}(\vec{x}'+s\vec{x}')\vec{\xi}'\right)d^2\vec{\xi}'$$

$$\vec{H}(\vec{x}',w) = \frac{w}{2\pi}\int_{-\infty}^{\infty}(\vec{x}'-\vec{\beta})\exp\left(iw\left(\tau-\frac{\vec{x}'\cdot\vec{r}}{c}\right)\right)d\tau \qquad (1)$$

For the thick beam with energy spread, the brilliance is the convolution product between $B(\vec{x},\vec{x}',s,w)$ and electron beam density function. The brilliance tuning curves of ID photon sources at the projected in the first-stage of HEPS in Figure 1.

Figure.1: Brilliance tuning curves of all kinds of IDs planed in HEPS first stage.

ID EFFECTS ANALYSIS

Beam Dynamics Perturbation Caused by Ideal IDs

In contrast to conventional accelerator magnets, undulators have a complicated three dimensional field distribution which the direction of vector potential is not always along the longitudinal axis as usual. The dynamic behavior of electron is dominated by the periodic undulator magnetic field. These effects are usually called dynamic kicks or 2nd order kicks because they scale inversely with the square of the particle energy.
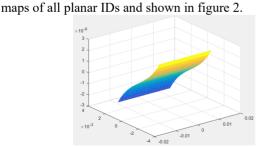
A Taylor expanded generating function of undulator magnetic field is developed to create a symplectic mapping routine for particle tracking [5]. It is a solution of Hamilton-Jacobi equation. This method allows as large integration step size as several undulator periods. However, it is required to supply an analytical representation of the magnetic vector potential which can be differentiated and integrated.
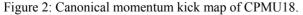
The implicit formulation of transformation of 2nd order map routine is derived as:

$$x_f = -\frac{\partial F_3}{\partial p_{xf}} = x + p_{xf}s - f_{101}x_3$$

$$p_x = -\frac{\partial F_3}{\partial x} = p_{xf} - f_{101x}p_{xf}x_3 - f_{011x}p_{yf}x_3 - f_{002x}x_3^2 - f_{001x}x_3$$

$$y_f = -\frac{\partial F_3}{\partial p_{yf}} = y + p_{yf}s - f_{011}x_3$$

$$p_y = -\frac{\partial F_3}{\partial y} = p_{yf} - f_{101y}p_{xf}x_3 - f_{011y}p_{yf}x_3 - f_{002y}x_3^2 - f_{001y}x_3 \tag{2}$$

Where $x_3 = 1/B\rho$ and $F_3(x, p_x, y, p_y, s)$ is the third form of the canonical transformation. f_{ijk} derived by inserting the Taylor series expansion of generation function $F_3 = \sum_{ijk} f_{ijk}p_{xf}^i p_{yf}^j x_3^k$ in HJE and solve the s-derivatives of f_{ijk} iteratively by making each individual expansion term to be zero. For the wide pole hybrid horizontal planar undulator, the scalar potential can be expressed as single harmonic Halbach expansion with $kx=0$. If we get for the field dependent f_{ijk} terms integrated over N periods $z_f = N\lambda$, the only nonzero term is:

$$f_{002} = -z_f B^2 cosh^2(k\, y)/(2k)^2 \tag{3}$$

2nd kick map of CPMU18 is derived as an example of maps of all planar IDs and shown in figure 2.

Figure 2: Canonical momentum kick map of CPMU18.

For any type of non-planar PM undulator such as EPU, it consists of several magnet rows. Each of the row also follow the Halbach condition[5]:

$$B_x = \sum_{i=0}^{n}\sum_{j=1}^{m}\frac{k_{xi}}{k_{yi,\tilde{j}}}c_{i,\tilde{j}}\sin(k_{xi}x)\exp(-k_{yi,\tilde{j}}y)\cos(k_{\tilde{j}}z + \varphi)$$
$$\times \exp(-k_{yi,\tilde{j}}\Delta g/2)$$

$$B_y = \sum_{i=0}^{n}\sum_{j=1}^{m}c_{i,\tilde{j}}\cos(k_{xi}x)\exp(-k_{yi,\tilde{j}}y)\cos(k_{\tilde{j}}z + \varphi)$$
$$\times \exp(-k_{yi,\tilde{j}}\Delta g/2)$$

$$B_z = \sum_{i=0}^{n}\sum_{j=1}^{m}\frac{k}{k_{yi,\tilde{j}}}c_{i,\tilde{j}}\cos(k_{xi}x)\exp(-k_{yi,\tilde{j}}y)\cos(k_{\tilde{j}}z + \varphi)$$
$$\times \exp(-k_{yi,\tilde{j}}\Delta g/2)$$

$$\tilde{j} = 1 + l(j-1) \qquad k_{xi} = k_{x1}i = (2\pi/\lambda_{x0})i$$

$$k_{yi,\tilde{j}} = \sqrt{k_{\tilde{j}}^2 + k_{xi}^2} \qquad k_{\tilde{j}} = k\cdot\tilde{j}. \tag{4}$$

The Fourier coefficients $c_{i,j}$ can be obtained by fitting with the numerical result of magnet field that generated by other simulation codes such as RADIA. Furthermore, a parameterization of the field of one individual magnet row permits the extrapolation of the fields of the complete undulator by linear superposition of the contribution from all the rows.

2nd order Kick-map of EPU73 is obtained by applying the method described above. Totally 40 Fourier coefficients per undulator are used for fitting. The kick results of 4-periods are shown in Figure 3.
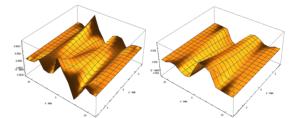

Figure 3: 4-periods kick-map of EPU73 in the horizontal direction(left) and vertical direction(right).

The 2nd kick maps of amount of 14 IDs was obtained and applied in the particle tracking program 'Accelerator Toolbox'. It was found that the maximum vertical tune shifted by 0.01 and the maximum vertical beta beat of 0.3% as referred in figure 4 due to 14 IDs in the ring. As the result, the linear perturbation cause by the ideal insertion devices could be negative.
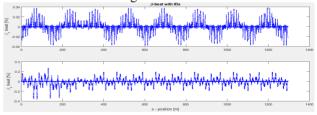

Figure 4: Horizontal and vertical beta beating with 14 IDs.

Frequency map analysis of HEPS storage ring with 14 IDs has also been token. It indicated a significant reduce of dynamic aperture in vertical direction as shown in Fig. 5.
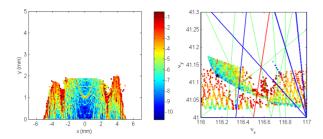
Figure 5: Dynamic aperture and tune footprint with 14 IDs at dp=0.

ID Field Integral Error Effects

As used in real case, some static field errors of insertion device should also be considered.

The main beam performance requirements from which ID field quality specifications can be inferred is local orbit stability. These requirements are derived from the need for the beam to be stable to within 10% of its rms size and divergence during the gap scans from maximum to minimum. [6]This mean the requirement of dx<2.3μm, dx'<0.26μrad, dy<0.42μm, dy'<0.14μrad which is one magnitude smaller than that of third generation light source in the horizontal direction. It is important to interpret this requirement as a stability requirement but not a requirement of the maximum deviation of close orbit in insertion devices. i.e. the requirement limits the variation range of beam position and angle during the gap scanning.

There are two pairs of BPMs with the tolerance of 0.1μm and correctors at the both side of straight section respectively applied for the local orbit correction as shown in Fig. 6:

Figure 6: Lattice with BPMs and correctors nearby the straight section.

Where the black square represent to corrector and the black rhombus represent to BPM. In addition, the misalignment is the other source of error which has to be considered. It has been set to 2μm for the horizontal and vertical position error and 2μrad for the horizontal and vertical divergence error.

The orbit correction result indicated that the orbit perturbation outside the straight section can be completely compensate if the horizontal and vertical first field integrals are both less than 700Gs.cm and the second field integrals are both less than 120000Gs.cm^2. Even so, there remains the internal orbit offset that can not be corrected by the global correction system. It will lead to the variation of photon beam position and angle during the gap scanning of ID. This limits the variation range of average orbit offset i.e. the field integral inside the ID. The requirements of the gap dependent field integral differential specifications are summarized below.

Table 2: Field Integral Differential Requirements

	Vertical field	Horizontal field
First field integral	30 Gs.cm	15Gs.cm
Second field integral	8000Gs.cm^2	1000Gs.cm^2

More in-depth simulation about the real-time orbit feedback considering the frequency dependence of the correction effectiveness still need to be taken in future.

ID Effects on Emittance

When considering the real case, insertion devices effect on emittance by two ways. Close orbit and optical perturbation due to the field and alignment error of IDs cause the emittance increase in general. An additional damping effect and quantum excitation modifying the equilibrium emittance is the other way. Thus we separate these two effects during the calculation at present. Ohmi-envelope method[7] is applied to calculate the emittance with all IDs installed in the ring but ignore their radiation effects at first. It is found that after the beam orbit correct the equilibrium emittance change can be ignored if the integral quadrupole and skew quadrupole field error of IDs less than 50G. The remaining effect is as damping wiggler which can be calculated immediately[8]. It is obtain that the horizontal emittance reduced from 59.6 pm.rad to 36 pm.rad due to the damping wiggler effect.

REFERENCES

[1] Toru Hara, Takashi Tanaka, and Hideo Kitamura, "Cryogenic permanent magnet undulators", *Phys. Rev. ST Accel. Beams*, vol. 7, p. 050702, 2004.

[2] Sasaki, S., "A new undulator for generating variably polarized radiation", *Jpn. J Appl. Phys*. 1992. Vol. 31, pp. L1794-L1796.

[3] Kim K. J., "Brightness, Coherence and Propagation Characteristics of Synchrotron Radiation", *Nucl. Ins. Meth. Phys. Res*. Elsevier Science Publishers, 1986, Vol. A, p.246.

[4] Elleaume P., "Undulators, Wigglers and Their Applications", edited by H. Onuki and P. Elleaume, London : Taylor & Francis, 2003, p. 38.

[5] Johannes Bahrdt, Godehard Wüstefeld, "Symplectic Tracking and Compensation of Dynamic Field Integrals in Complex Undulator Structures", *PRST-ab*, Vol. 14, p.040703(2011).

[6] Y. C. Chae and G. Decker. "Advanced Photon Source Insertion Device Field Quality and Multipole Error Specification", in *Proc. PAC 1995*, pp. 3409–3411.

[7] Kazuhito Ohmi, Kohji Hirata, and Katsunobu Oide, "From the Beam-Envelope Matrix to Synchrotron-Radiation Integrals", *Phy. Rev. E*, Vol.49, no. 1, p.751, Jan. 1994.

[8] Wu Chao, "Accelerator Physics and Engineering", edited by Wu Chao, Maury Tigner, Singapore, 1998, p. 189.